Developing acceleration schedules for NDCX-II*

W. M. Sharp, A. Friedman, D. P. Grote
Lawrence Livermore National Laboraatory, Livermore, CA, USA
E. Henestroza, M. A. Leitner, W. L. Waldron
Lawrence Berkeley National Laboratory, Berkeley, CA, USA

Abstract

The Virtual National Laboratory for Heavy-Ion Fusion Science is developing a physics design for NDCX-II, an experiment to study warm dense matter heated by ions near the Bragg-peak energy. Present plans call for using about thirty induction cells to accelerate 30 nC of Li^+ ions to more than 3 MeV, followed by neutralized drift-compression. To heat targets to useful temperatures, the beam must be compressed to a millimeter-scale radius and a duration of about 1 ns. An interactive 1-D particle-in-cell simulation with an electrostatic field solver, acceleration-gap fringe fields, and a library of realizable analytic waveforms has been used for developing NDCX-II acceleration schedules. Axisymmetric simulations with WARP have validated this 1-D model and have been used both to design transverse focusing and to compensate for injection non-uniformities and radial variation of the fields. Highlights of this work are presented here.

1. Introduction

The Virtual National Laboratory for Heavy-Ion Fusion Science is developing a physics design for NDCX-II [1], an experiment to study warm dense matter (WDM) heated by ions near the Bragg-peak energy. To minimize the cost of this facility, induction cells and other hardware from the decommissioned Advanced Test Accelerator (ATA) at Lawrence Livermore National Laboratory will be reconditioned and reused. Present plans call for using about thirty ATA cells to accelerate 30 nC of Li^+ ions to an energy in excess of 3 MeV before neutralized drift-compression. To heat targets to useful temperatures, the beam must be compressed to a sub-millimeter radius and a duration of about 1 ns, a longitudinal compression factor of more than 600.

Developing a suitable acceleration schedule for NDCX-II is challenging for several reasons: (a) The limited floor space constrains the number of acceleration cells to forty or fewer; (b) budgetary considerations necessitate the use of passive circuit elements to shape waveforms; (c) the applied waveforms must compensate for the beam longitudinal space charge and impose a head-to-tail velocity tilt, in addition to accelerating the beam; and (d) the need for extreme longitudinal and transverse compression requires minimal emittance growth and halo formation during acceleration.

A combination of 1-D particle-in-cell simulation and more-realistic axisymmetric modeling is being used to develop NDCX-II acceleration schedules. This paper first reviews a class of acceleration schedules worked out using an interactive 1-D particle code and demonstrates that the essential features of these results are retained in axisymmetric simulations using the particle-in-cell code WARP [2]. More recently, the 1-D code has been used to develop a modified NDCX-II design that takes into account the variation in initial beam energy that is expected from the injector. We present preliminary WARP simulations of this modified design beginning at the injector, and we briefly discuss future work to refine the NDCX-II physics design.

2. Validation of the 1-D model

In another paper [1], we discuss a 1-D particle-in-cell code developed to explore NDCX-II lattice layouts and acceleration schedules that optimizes the cell parameters. The code, which is written in Python, uses a leapfrog advance and includes a simple 1-D electrostatic field solver [3] that gives a close approximation to the longitudinal component of the space-charge field of a beam with uniform radius and charge density. Waveforms at induction gaps can be chosen from a library of realizable analytic waveforms, read from tables, or calculated from circuit models. An important aspect of the code is that it automatically adjusts each waveforms to match the duration of the beam as it enters the gap and to respect user-specified limits on the induction-module voltage and volt-seconds. An

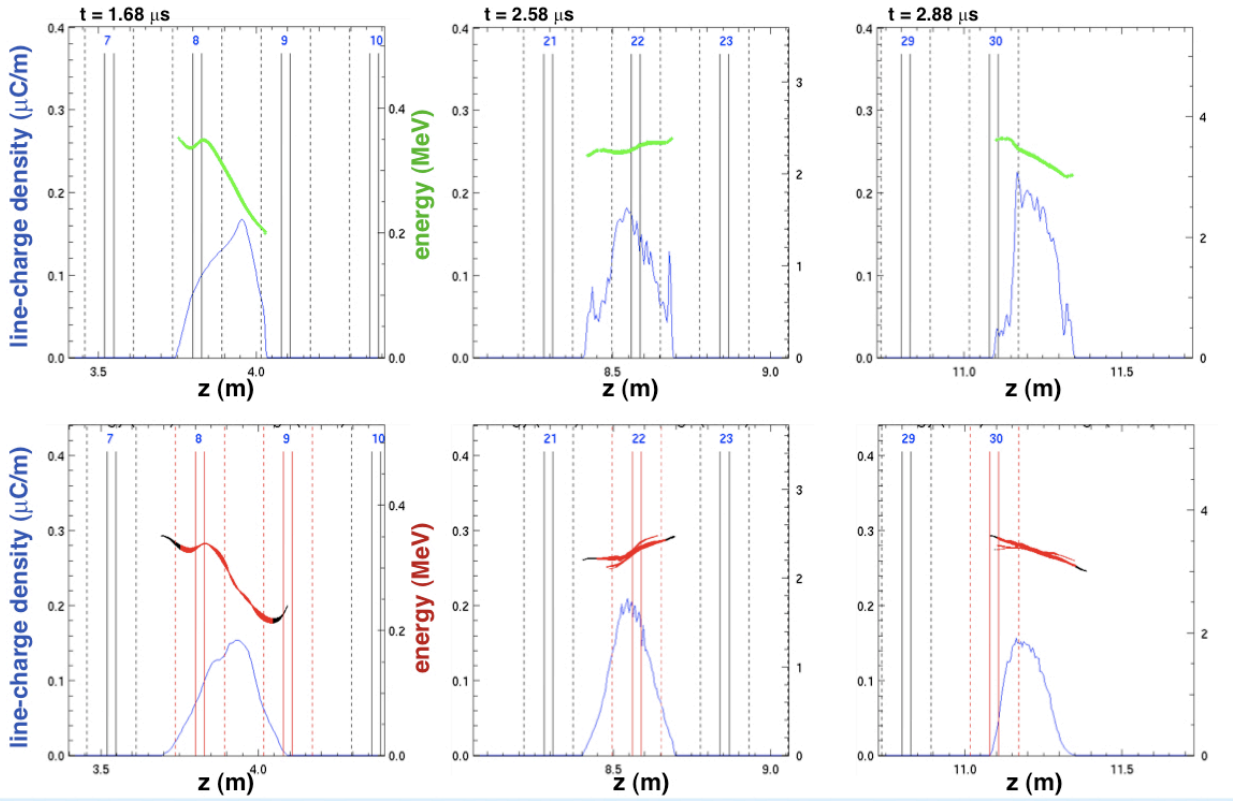

Figure 1. Longitudinal phase space and line-charge density at selected times from the 1-D code (above) and an axisymmetric WARP simulation (below). The solid vertical lines indicate physical gap boundaries and dashed lines mark the axial locations where the gap field has decreased to 2.5% of its maximum value.

optimizer built into the code can choose waveform parameters to produce a beam distribution with minimal short-wavelength non-uniformities and deviations of $\langle v_z \rangle$ from linearity in z. In addition, specified cells can apply an appropriate voltage to control expansion of the beam ends. After the acceleration lattice, the space-charge field can be reduced smoothly to zero over an arbitrary distance to model the effect of a neutralizing plasma, providing an estimate of the longitudinal focal length and minimum beam length.

Ref. [1] presents a family of lattice layouts and acceleration schedules for NDCX-II developed using this 1-D particle code. The main features of the conceptual design are (a) an "accel-decel" injector to produce a 550-ns beam of 100-keV Li^+ ions [2], (b) a compression section that imposes an head-to-tail velocity variation or "tilt" and allows the beam to compress longitudinally as it drifts, (c) an acceleration section that alternates flat-topped waveforms that increase beam energy and triangular pulses that maintain the velocity tilt, and (d) a neutralized drift section in which the beam reaches its minimum length as it is compressed radially by a strong solenoid. The particular case presented here has thirty induction gaps, grouped in blocks of five and separated by drift sections of various lengths. Except for two induction cells in the first ten used to control the longitudinal space charge, referred to here as "ear" cells, all the waveforms are simple and can be generated using elementary pulse-forming circuits. The initial compression decreases the beam duration to less than 70 ns, allowing the use of the 200-kV ATA Blumleins for the final 20 induction cells. As it exits the last gap, the beam has an average energy of 3.4 MeV and an 8% head-to-tail velocity tilt, allowing it to compress to a 1-ns duration with a 2.4-m focal length. We find that these results are not highly sensitive to details of lattice and waveforms. However, the original 6.7-cm radius of the ATA beam pipe proved to be unusable, due to the fringing of the gap fields. The physical gap length of the ATA induction modules is 2.8 cm, but with the original pipe radius, the distance between the points where the gap field drops to 2.5% of its maximum value is 26.4 cm along the axis. which is only slightly shorter than the 28-cm lattice period. With fringes of that size, gap transit times were so large that we could find no acceleration schedule with fewer than forty cells that

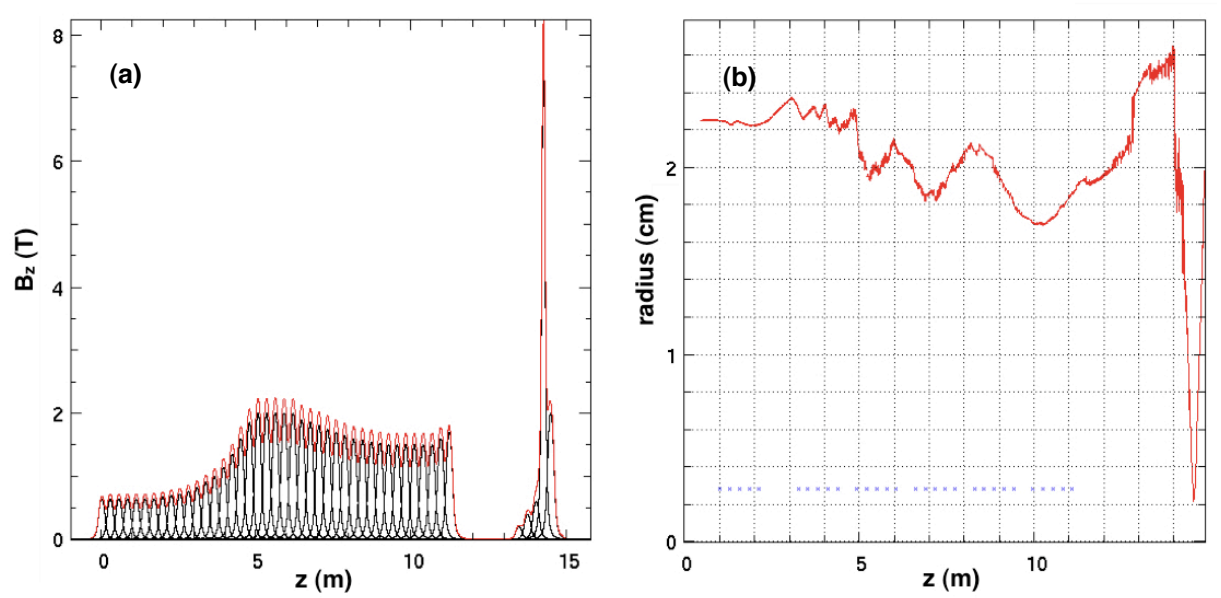

Figure 2. (a) On-axis focusing field and (b) calculated edge radius from an axisymmetric WARP simulation of a 30-nC L^+ beam initialized in equilibrium. The acceleration waveforms were obtained from a 1-D simulation of the same beam and lattice. The small blue "x"s mark the axial centers of the thirty induction gaps in this simulation.

achieved the minimal 3-MeV final energy. Consequently, all the schedules discussed here use a 4-cm beam-pipe radius, which gives the gap fringe fields an edge-to-edge length of about 15 cm along the axis.

We have carried out axisymmetric simulations with the WARP particle-in-cell code to validate the 1-D code. The beam is initialized with the same ion energy and current profile as the 1-D code, An initial angular velocity in order to allow us to start the simulation with the beam in transverse equilibrium. For a space-charge-dominated beam, a B_z field of about 0.56 T and an angular frequency of 3.96 x 10^6 s^{-1} is found to give an edge radius $r_b^2 = 2 \langle r^2 \rangle$ of 2.5 cm, as assumed in the space charge model in the 1-D code. The solenoid strengths along the accelerator are then chosen to maintain that radius approximately as the beam accelerates and compresses, and a strong solenoid (8-15 T) is positioned near the focal plane to compress the beam radially.

With this initialization, WARP simulations reproduce the gross features of 1-D results obtained with the same lattice and waveforms. Fig. 1 shows the current and longitudinal phase space at selected times for the two codes. Although WARP results reproduce the qualitative features calculated by the 1-D code, the beam is systematically longer than that predicted by the simpler model, making the line-charge density correspondingly lower, and the final velocity tilt is less. These differences suggests that the 1-D space-charge model underestimates the self field. Further study of the WARP simulation is needed to determine whether the underestimation results from approximations in the 1-D model, from the failure, seen in Fig. 2, to maintain a constant beam radius, or from radial variation of the gap fringe fields. One result of the reduced velocity tilt is that the WARP beam has a duration at best longitudinal focus of about 2 ns, compared with less than 1 ns predicted by the 1-D model, although this time scale is not well-resolved in either simulation. A second result is that this focal plane is 3.4 m beyond the last acceleration gap, a focal length that is nearly 0.9 m longer that the value expected from the 1-D code. The 8-T final-focus magnet used in this simulation produces a 2-mm focal-spot edge radius, about a factor of four larger than needed for WDM experiments. We can reduce this focal spot to about 1-mm by using a 15-T solenoid, however, and we expect that some further improvement can be achieved by more careful manipulation of the beam in the accelerator and by increasing the beam radius as it approaches the final-focus solenoid.

An important finding of this WARP simulation and similar ones is that the transverse emittance shows little secular growth during acceleration and compression, despite the severe changes in the longitudinal phase space. Fig. 3 shows the r-r' emittance, which removes the contribution of average rotation, as a function of longitudinal position z during acceleration and final focus. The plot shows considerable scatter but less than a factor of two

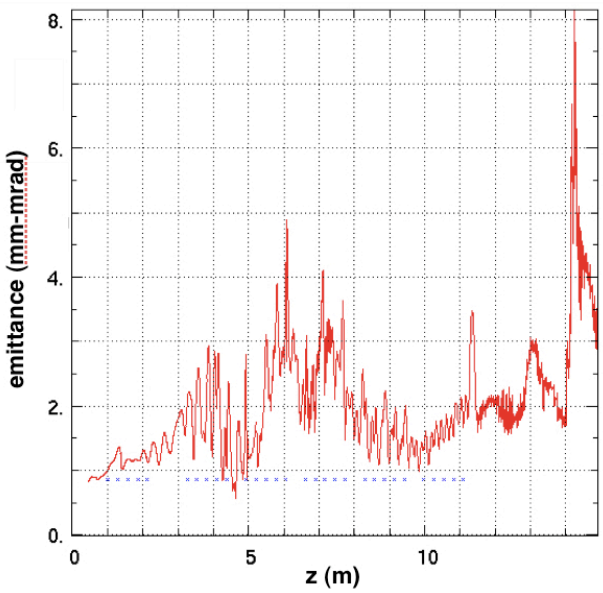

Figure 3. Evolution of the beam r-r′ emittance during an axisymmetric WARP simulation of a 30-nC L^+ beam initialized in equilibrium. The beam was initialized with an x-x′ emittance of 1 mm-mrad in the absence of bulk . rotation. The blue "x"s again mark the centers of the thirty induction gaps.

secular growth. If we assume that the NDCX-II injector can produce a beam with the 1-mm-mrad emittance assumed here, this limited emittance growth should allow final radial compression to the 0.5-mm edge radius required for WDM experiments.

3. Source-to-focus simulations

Extracting a pulse from a diode introduces the problem of a nonuniform initial beam energy. For an accel-decel injector of the sort that we plan to use for NDCX-II [4], WARP simulations show that the beam reaching the first acceleration gap has about an energy that is about 20% above the nominal energy at the head and drops off about 50% near the tail. If we try to accelerate a beam with this energy variation using the acceleration schedule discussed in Section 2, the final energy and compression are seriously degraded. The obvious solution is to remove the energy variation to the extent possible in the first gap, then accelerate and compress as before. However, the energy deviations at the ends occur over about 50 ns, while the time it takes a 100 keV Li ion to traverse the gap field is nearly 100 ns, due to the considerable fringing of the gap fields. Consequently, the beam-energy variation as the pulse enters the first gap cannot be accurately removed. Instead, we average the deviation of the energy of particles in the gap, suitably weighted by the spatial envelope of the gap field, and construct an approximate correction field from this data. The correction replaces the rise and fall with energy undulations of about ±7% at the ends. Due to this residual energy fluctuation, the ends compress less than in the uniform-energy case, leading to a somewhat longer beam and reduced velocity tilt. To compensate for these changes, longer drift sections are inserted between the first three cell blocks, and the early tilt cells are reoptimized. The result is a thirty-cell lattice that is 0.56 m longer than the earlier design, but produces a beam with nearly the same energy, focal length, and final duration.

To date, the WARP simulations based on this modified acceleration schedule are not nearly as successful as the uniform-energy cases. Plots of the longitudinal distribution function at three time are shown in Fig. 4, along with the corresponding beam currents. For this simulation, we use the 102 keV acel-decel injector reported previously [4] and specify solenoid strengths that are similar to those shown in Fig 2a. Unlike the corresponding 1-D case, the WARP distribution is seriously distorted as it exits the acceleration lattice, leading to poor final compression. At the point of best longitudinal focus, the bulk of the WARP beam charge is in a 10-cm long "foot" that precedes a 1-ns current spike. Since we have already demonstrated that the 1-D code adequately represents the full axisymmetric

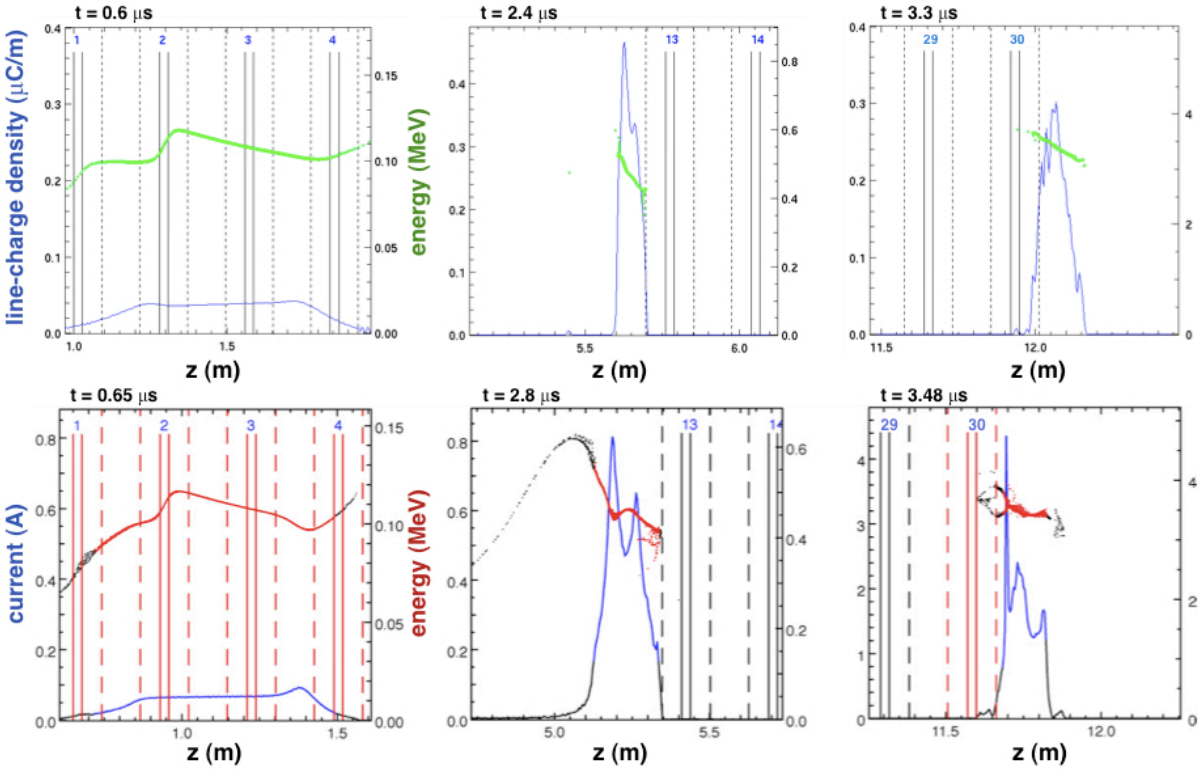

Figure 4. Longitudinal phase space and beam current at selected times for a 1-D beam with a nonuniform initial energy (upper) and an axisymmetric WARP simulation with the beam initiated by emission from a cathode (lower). The solid vertical lines indicate physical gap boundaries and dashed lines mark the axial locations where the gap field has decreased to 2.5% of its maximum value.

physics in comparable cases, we must look elsewhere for the causes of the differences seen in this case. One likely problem is that the 1-D simulation was initialized with a qualitatively similarly energy variation, rather than one reconstructed from the WARP simulation of the NDCX-II injector. The effects of this discrepancy cannot be estimated due to the complicated particle dynamics. The second likely cause of the difference is the rather poor transverse match for this case. After entering the solenoid lattice, the calculated edge radius of the WARP beam initially oscillates between about 1.5 cm and 2.8 cm with a period of nearly 1 m. The absence of an initial transverse match violates the assumption in the 1-D model of a uniform radius and may account for the fluctuation-averaged emittance being more than double what would be expected for a 1-eV source temperature.

4. Summary

The early WARP simulations of NDCX-II presented here encourage optimism that a physics design can be found that meets all the cost and operational requirements. Comparisons of 2-D WARP runs using the same layout and waveforms as our interactive 1-D design code show only small differences, suggesting that the strategy, described in Ref [1], of rapid compression followed by acceleration will work in practice. We find that solenoids with strengths of 2 T or less appear adequate for transverse focusing, and despite the aggressive initial compression, the growth of transverse emittance during acceleration is modest, so that the beam can be focused to a 1-mm rms spot radius by an 8-T solenoid.

The results presented here, of course, represent just the first steps toward a complete NDCX-II physics design. Further work with the 1-D code is needed to reduce the phase-space distortion after initial compression and to

increase the final energy and current. In WARP simulations, we plan to use the *r-z* envelope model to improve initial transverse matching, maintain a uniform radius during acceleration, and minimize the focal spot. Time-dependent focusing solenoids may be needed to reduce chromatic aberration. WARP will also be used to explore injector alterations that might increase current and improve beam quality. For example, we could increase the current by using a larger cathode and a greater extraction voltage, and we might find it advantageous to extract a shorter beam by removing more of the initial beam energy in the accel-decel structure. A realistic neutralizing plasma will be used in some of these runs in place of the phenomenological neutralization now employed to verify that the beam is stable in the neutralized-drift region and insensitive to plasma non-uniformities. Finally, 3-D WARP simulations are needed to determine the tolerances to errors in the lattice alignment, the beam distribution, and the acceleration and longitudinal-control waveforms.

Acknowledgments

This work was performed under the auspices of US Department of Energy by LLNL under Contract DE-AC52-07NA27344 and by LBNL under Contract DE-AC03-76SF00098.

References

[1] A. Friedman, *et al.,* "Toward a physics design for NDCX-II, a ion accelerator for warm dense matter and HIF target physics studies," in these *Proceedings*.
[2] D. P. Grote, A. Friedman, I. Haber, W. Fawley, and J.-L. Vay, *Nucl. Instr. and Meth. A* **415**, 428 (1998).
[3] J. J. Barnard, G. J. Caporaso, S. S. Yu, and S. Eylon, "One Dimensional Simulations of Transients in Heavy Ion Injectors," *Proc. 1993 Part. Accel. Conf.,* Washington, DC, 17-20 May 1993, pp 712-714.
[4] E. Henestroza, S. S. Yu, J. W. Kwan, and R. J. Briggs, "Extraction and compression of high line-charge density ion beams," *Proc 2005 Part. Accel. Conf.*, IEEE 0-7803-8859-3, Knoxville, TN, 16-20 May 2005.